Calculation Of Heat Transfer Coefficient Of Cuo (Copper Oxide) Produced As Nanofluid And Creation Of Predictive Model

Ahmet Beyzade Demirpolat[1*], Aydın Çitlak[1], Mehmet Daş[2]

[1]engineering Faculty, Mechanical Engineering, Firat University, 23100 Elazig, Turkey
[2]ilic Dursun Yildirim V.H.S., Erzincan Binali Yildirim University, 24700 Ilic, Erzincan, Turkey
Corresponding Author; Ahmet Beyzade Demirpolat

Abstract: *It is important to be able to use the energy in a more beneficial way by increasing the heat transfer in the in-pipe flows. Because, with the technological developments, there is an increasing energy demand in the industry sector. For this reason, researchers have been working on new generation heat transfer fluids in recent years. In this study, CuO (copper oxide) nanoparticle production was performed. SEM image analysis and ultraviolet - visible light (UV-Vis) analysis showing that the material produced has a nano material characteristic was performed. Heat transfer coefficients (h) were determined using pure water, ethanol and ethylene glycol materials together with CuO nanoparticles. It was observed that the number of Reynolds changes between 846 and 2292 in the experiments performed. A predictive model was obtained by using the decision tree regression for the calculated heat transfer coefficient of nanofluid. The mean absolute error (MAE), root mean squared error (RMSE), relative absolute error (RAE) and root relative absolute error (RRAE) analyzes were performed for the predictive model in decision tree regression.*

Keywords - *Nanofluid, nano material, heat transfer coefficient, decision tree regression*

I. INTRODUCTION

In our daily life, we encounter the flow in circular and non-circular pipes. The hot and cold water we use in our homes is pumped through the pipes. City water is distributed with an expensive pipe network. Oil and natural gas are transported by hundreds of kilometers of pipelines. Blood in our body is carried by arteries and veins. The cooling water in the engine is transported to the pipes in the radiator which is cooled while flowing through the hoses by means of hoses. Most fluids, especially liquids, are transported by circular pipes [1]. It is important to be able to use the energy in a more beneficial way by increasing the heat transfer in the in-pipe flows. Because, with the technological developments, there is an increasing energy demand in the industry sector in recent years. Energy demand, which is one of the most important inputs of daily life, is continuously increasing and energy resources are rapidly consumed. In this respect, it is of great importance to revise existing energy conversion systems and to develop new methods in order to benefit more from the limited energy resources available [2]. Today, nano technological developments have allowed the production of particles in nanometer dimensions, thus adding particles into the fluid. In particular, the techniques used in the production of metallic nanoparticles; micro emulsion technique, gas phase production technique, inert gas condensation, chemical vapor condensation and hydrogen reduction technique [3]. By incorporating the nanoparticles into the working fluid, the performance of heat transfer is significantly improved [4]. Nanoparticles, nanofibres, nanotubes and other nanomaterials are produced primarily as a dry powder by physical methods or chemical methods. Then, these nano-sized powders are dispersed in water, the basic fluid. In order to stabilize the particles in the fluid and to obtain a homogenous distribution, the processes such as magnetic mixing, ultrasonic mixing, high shear mixing are applied [5].

Nanoparticles that help improve heat transfer; In the effect on the properties of nanofluid, it is very important to prepare the nanofluids, the thermophysical properties of nanofluids and the heat transfer measurement techniques correctly. Zhu et al. [6] obtained non-agglomerated and stable Cu nanofluids with $CuSO_4 \cdot 5H_2O$ and $NaH_2PO_2 \cdot H_2O$ by one-step method. The thermal conductivity of nanofluid prepared with Cu and ethylene glycol of 0.3% volumetric ratio was 40% improvement. Eastman et al. [7] is a one-step method for producing nanostructures containing various nanoparticles such as TiO_2, CuO and Cu. This method has also been used to synthesize sub-nanoparticles [8]. In this method, the nanoparticles are heated by the heat obtained from the electrode and then condensed into the liquid chamber in the vacuum chamber to produce nanofluids. The thermos physical properties of nanofluids are very important for heat transfer applications. The thermophysical properties contain different parameters. These; specific heat capacity, viscosity, thermal conductivity and heat transfer coefficients. Heat transfer of nanofluids is best analyzed by heat transfer

coefficient [9]. Nguyen et al. [10] studied the nanofluid composition of aluminum-water to see the effect of particle size on viscosity. In their study, they obtained the same results for particles with 36 and 47 nm in 4% volumetric ratio. They stated that the higher the particle size, the higher the viscosity, and the more viscosity of the fluid.

Because the solid conductivity of the solid metals is higher than the basic fluid, the small solid metals introduced into the fluid increase the thermal conductivity [11]. Xie et al. [12] have observed the effect of particle size on the thermal conductivity by producing a particle size of 26 to 600 nm of non-oxide ceramic nanoparticated, nanofluid (SiC) and Al_2O_3 nanoparticle having a particle size of 1.2 to 3.02 nm.

Decision tree regression is a computational intelligence method such as artificial neural network. Artificial Neural Networks (ANN) are briefly developed by inspiring the human brain; parallel and distributed information processing structures are composed of process elements connected by means of weighted links and each having their own memory; in other words, computer programs that mimic biological neural networks [13]. In the literature, there are several studies related with the estimation of nanofluids properties by ANN. Uysal and Korkmaz, in the rectangular cross-section, the quantitative analysis of Ag-MgO / water hybrid nanofluidic flow by convective heat transfer and entropy production characteristics. The Reynolds number ranged from 200 to 2000. Ag-MgO / water used Artificial Neural Networks to predict entropy production of hybrid nanofluidic flow [14]. In their study, Kılıç et al. Investigated the quantitative investigation of heat transfer and fluid flow from a heated surface, using nanofluids and pulsed jets. They obtained a predictive model in ANN with the obtained values [15].

Our work, CuO nanoparticles were produced and then SEM images of the produced particles analysis and ultraviolet - visible light (UV-Vis) analysis were carried out. Nanofluids were obtained by using Nano particles produced with Pure Water, Ethanol and Ethylene Glycol materials and experiments were carried out to determine the heat transfer coefficients by passing the fluid through the experimental setup. In all experiments, the Reynolds number ranged from 846 to 2292. For the heat transfer coefficient obtained for CuO, a predictive model was created by using decision tree regression. The error analysis of the predicted model was performed.

II. MATERIAL AND METHOD

In this study, heat transfer coefficients were calculated after the production of a nanofluid at different pHs. For predicted heat transfer coefficients, a predictive model was developed by using decision tree regression.

2.1 CuO Nanofluid Production

CuO particle production 3.633 grams (0.02 mol) Copper Acetate dissolved in 100 ml ethanol in ultrasonic bath for 30 minutes and the solution formed. 8 grams (0.2 mol) of NaOH (Sodium Hydroxide) in 200 ml of distilled water was then dissolved in an ultrasonic bath for 30 minutes. The resulting mixtures were then combined and stirred in the magnetic stirrer for 1 hour. In order to obtain the mixture at different pH ratios, ammonia was added to the mixture with 10 ml beaker to obtain mixtures at different pH ratios. The mixture was allowed to settle for 20 hours after preparation. After the resting process was completed, filter paper was placed in the funnels and the material was subjected to drying at 50 °C, and the resulting material was heat treated at 450 °C for 1 hour. SEM images of the material produced, FTIR (Fourier Transform Infrared Spectroscopy) Analysis, X-ray diffraction method analysis (XRD), X-ray spectroscopy (EDS or EDX) analysis, Ultra-violet visible light (UV-Vis)) and Thermogravimetry (TG) Differential Thermal (DTA) analysis measurements were performed and nano particle production was found to be successful.

Materials used for the production of nanofluids after production of nanoparticles; 57.1% Pure Water, 28.6% Ethylene Glycol, 14.8% Ethanol and nano materials produced in 0.1% of the mixture of nano particles are added after 45 minutes in an ultrasonic mixer by mixing the mixture in an additional 15 minutes in a fish mixer to be used in the nanoactive test setup has become available. The pH values determined for the nanoparticles are varied before the production of CuO nanofluids at different pHs. The reason for this is the change in the content of the fluid produced since different materials are used when producing nano fluid.

After determining the density of the produced nanofluids, the pH of the nanofluids produced in the pH meter is determined. Experiments were performed for 5 different Reynolds values between 846 and 2292 values for the produced nanofluids and the temperature values of the fluid at 5 minute intervals from the inlet, outlet temperature and pipe surface were measured with the help of Thermo Couples until the temperatures were stable. Heat transfer coefficient and heat transfer coefficients were calculated with the obtained data. The experimental set-up for the heat transfer coefficient calculation is shown in Figure 1.

Fig.1 Data-logger unit for monitoring solar PV plants

1-Pump, 2-T Connection reducer elbow pipe, 3-Heat Band, 4 -Copper pipe, 5-Plastic pipe 6- Flow Measurement Electronic device sensor, 7-Flow Measurement Electronic device, 8-Fluid reservoir, 9-Flow Adjustment Valve, 10-Fluid Thermometer and 11-Thermocouple

As shown in Fig. 1, the flow rate of the flow rate is adjusted by means of a flow rate control valve. Temperature measurements were taken from 4 different points on the surface of the pipe with the help of the thermocouples of the nanofluids passing through the copper pipe through laminar flow. The inlet and outlet temperatures of the nanofluid to the copper tube were measured by means of a fluid thermometer. The volume flow rate of the nanofluid was determined by means of the flow meter.

2.2 Heat Transfer in Nanofluids

Heat transfer between all environments and environments where there is a temperature difference occurs. In the case of a stationary solid or a fluid, the term transmission is used when the heat transfer occurs because of the temperature difference. Furthermore, when a surface and a fluid in motion are at different temperatures, the heat transfer between them is referred to as the term transport. All surfaces with finite temperature emit energy in the form of electromagnetic waves. The heat exchange between two surfaces of different temperature, if there is no barrier to seeing each other, is called radiation [15].

The transmission indicates the energy transfer due to the temperature difference in an environment. Heat conduction can be fully explained by Fourier's law. A body having a fixed cross-sectional area; one dimensional, steady state heat transmission is expressed by the following equation.

$$q_x^{"} = -k \frac{dT}{dx}, q_x^{"} = -k \frac{T_2 - T_1}{L} \tag{1}$$

Transport is a combination of mass movement, the mixing of macroscopic parts of hot and cold fluid elements, heat conduction in the cooling medium, and energy storage. This is called natural (or free) convection if the charge forces due to the density differences caused by the lack of temperature in the fluid are associated with the convection event. Besides, flow; if it occurs with an external effect such as a fan, pump or atmospheric wind, this is called forced convection. Heat transfer from a hot object to the refrigerant fluid is associated with the following equation, known as Newton's Cooling Law [16].

$$q^{"} = h(T_s - T_\infty) \tag{2}$$

Investigators studying the effects of nanofluids on heat transfer have observed that not only thermal conductivity, but also the heat transfer coefficient, is too large in the nanocomposed fluid as in Figure 2. [16].
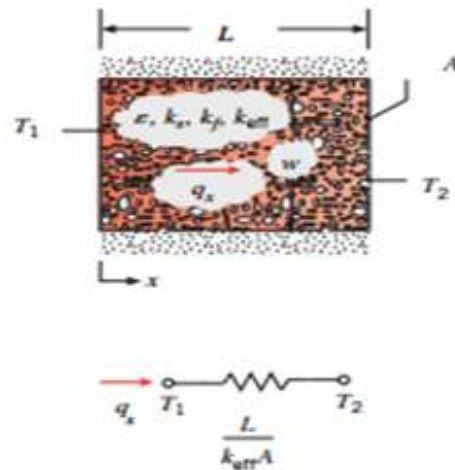
Fig.2 Heat transfer properties of nanofluids

To adapt the heat transfer properties of the suspension obtained with mixtures of liquids and solids, it can be formulated as follows.

$$q_x = \frac{k_{eff} A}{L}(T_1 - T_2)$$
(3)

If fluid motion is negligible, the above equation is valid when the heat transfer in the environment is neglected. Effective thermal conductivity at equality. Effective thermal conductivity varies with the porosity or volume fraction of the medium. In addition to these properties, it depends on the thermal conductivity of the solid and liquid. Experimental studies conducted by different researchers have shown that the increase in the heat transfer coefficient of the nanofluids is higher than the thermal conductivity in both laminar and turbulent flow conditions. The basic law of transport was declared by Newton before Fourier's transmission law was proposed, and it was named Newton's law of cooling.

$$Q = hA(T_w - T_f)$$
(4)

In the above formula, Q is the heat transfer between the wall and the moving liquid. A is the common surface area between solid and liquid. T_w is the average temperature of the surface and T_f is the average of the inlet and outlet temperature of the liquid [16].

In circular pipes; The Nusselt number is a constant in fully developed flow situations where laminar flow and constant surface heat flux (q_s = constant); It does not depend on Reynolds or Prandtl numbers [16]. The conductivity coefficient k value was calculated according to the following formula.

$$Nu = \frac{hD}{k} = 4.36$$
(5)

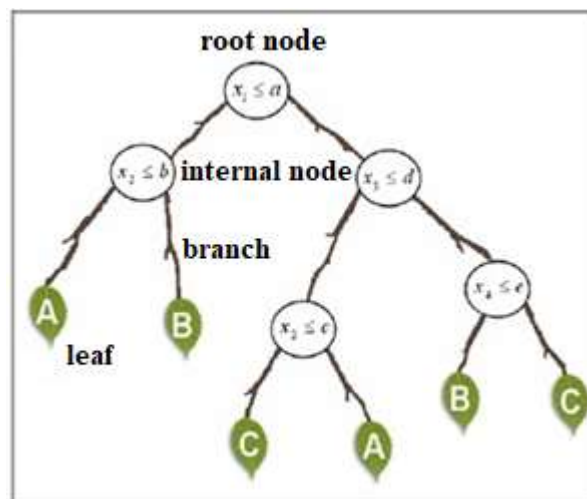**2.3 Scanning Electron Microscope Analysis**
Basically, the scanning electron microscope (SEM), Tungsten, Lantan hexane boron cathode or the field emission (FEG) from the day of the use of electrons emerging from the surface to be examined as a result of the interaction is based on the interaction. In general, this electron energy in SEM can range from 200-300 eV to 100 keV. For this purpose, the electron beam, which is collected by the concentrator electromagnetic lens (condenser lense), focuses on the lens lens and perform scanning on the sample surface with electromagnetic deflector coils. The formation of images in a scanning electron microscope is basically; it is based on the principle of collecting and examining the signals resulting from physical interactions with the surface of the electron beam (elastic, non-elastic collisions and others). In the SEM device, the electrons in the electron bundle are the secondary electrons that emerge as a result of the non-elastic collision with the atoms in the material (ie, transferring their energies to the electrons in the atoms on the sample surface). These electrons emerge from a depth of about 10 nm of the sample surface, and their typical energies are at most 50 eV. Secondary electrons are collected by means of the photomultiplier tube and associated with the scan signal location, for example, to obtain a surface image [17].

2.4 Ultraviolet and visible light (UV-Vis) Analysis

This is a measure of the decrease in light of a beam after it has passed through a sample or reflected from a sample surface. The decrease in intensity of light indicates that absorption is increased. For example, the concentration is measured by measuring the absorption of a specific wavelength. UV-Vis spectroscopy is often used to measure molecules or inorganic ions and complexes in solution. Molecules absorb UV or Vis wavelengths, different molecules absorb different wavelengths. Absorption spectra are composed of several absorption bands showing the structure of the molecule [18].

2.5 Modeling of Data with decision tree regression

Decision tree regression is a classification and pattern identification algorithm that has been widely used in the literature in recent years. The most important reason for the widespread use of this method is that the rules used to form tree structures are understandable and simple [19]. The basic structure of a decision tree consists of three basic parts called nodes, branches and leaves, as shown in Figure 3. In this tree structure, each attribute (Air velocity, Temperature etc.) is represented by a node. Branches and leaves are other elements of the tree structure. The last part of the tree and the upper part of the tree are called roots. The parts between the roots and leaves are expressed as branches [19]. In other words, a tree structure; a root node containing data, internal nodes (branches), and end nodes (leaves). The basic principle in constructing a decision tree structure by using the attribute information of the training data can be expressed as a series of questions about the data and concluding in the shortest time by acting on the answers obtained. In this way, the decision tree collects the answers to the questions and creates decision rules. The root node, which is the first node of the tree, begins to ask questions for the classification of the data and the structure of the tree, and this process continues until the nodes or leaves without branches are found [20].

Fig.3 Decision tree structure consisting of three classes with four-dimensional property space

In the system, decision tree regression was modeled as thirteen inputs and one output. Reynolds number (Re), duration (t), fluid velocity (V), hydrogen power value (pH), fluid inlet temperature (Tg), outlet temperature (Tc), inlet and outlet temperature average (Tavg1), (T1,2,3,4) surface temperature average (Tavg2) and heat conduction coefficient (k) of the fluid were used as inputs. The heat transfer coefficient (h) of the fluid is used as outputs information. The structure of the decision tree regression model is given in Figure 4.
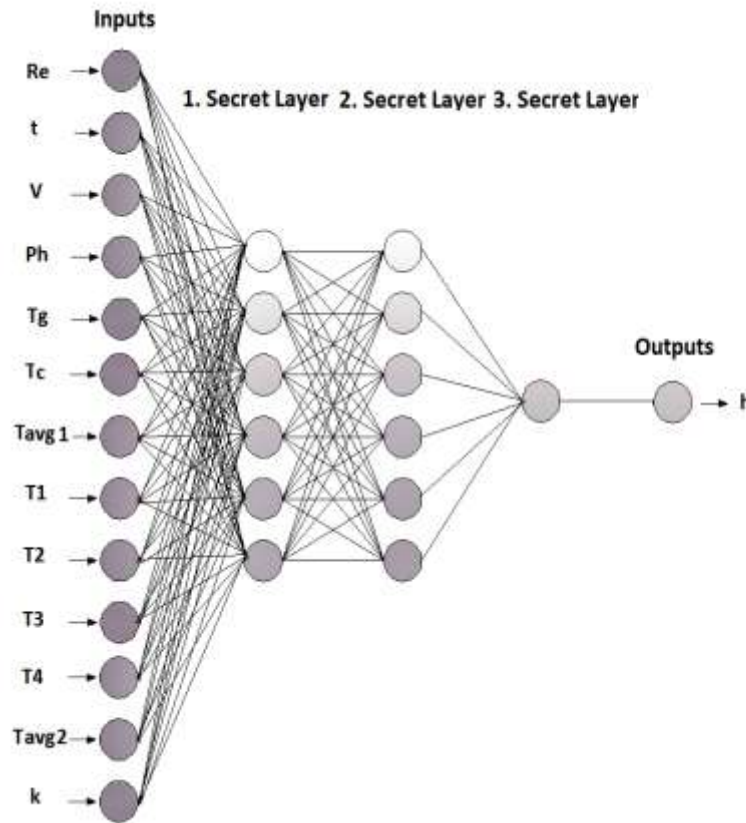
Fig. 4 Predictive model structure

MATLAB 2016a software is used for modeling of heat convection values with artificial neural network. The information set has 280 input and output information. Of these, 200 were used in the training process. 80 were used in the test procedure. MP5 algorithm is used in decision tree regression. The mean absolute error (MAE), root mean squared error (RMSE), relative absolute error (RAE) and root relative absolute error (RRAE) analyzes were shown in Table 1.

Table 1. Accuracy Criteria and Formulas

Accuracy Criteria	Formulas	Parameters
MAE	$$\dfrac{\left|P_1 - A_1\right| + ... + \left|P_n - A_n\right|}{n}$$	P: Predicted Value A: Actual Value n: Total Estimated Value
RMSE	$$\sqrt{\dfrac{\left(P_1 - A_1\right)^2 + ... + \left(P_n - A_n\right)^2}{n}}$$	P: Predicted Value A: Actual Value n: Total Estimated Value
RAE	$$\dfrac{\left|P_1 - A_1\right| + ... + \left|P_n - A_n\right|}{\left|A_1 - A'\right| + ... + \left|A_n - A'\right|}$$	P: Predicted Value A: Actual Value A': Average Of Actual Values
RRAE	$$\sqrt{\dfrac{\left(P_1 - A_1\right)^2 + ... + \left(P_n - A_n\right)^2}{\left(\left|A_1 - A'\right|\right)^2 + ... + \left(A_n - A'\right)^2}}$$	P: Predicted Value A: Actual Value A': Average Of Actual Values

III. RESULTS

In this study, the heat transfer coefficient of CuO nano fluids in various pHs for nano fluids obtained by using nanomaterials produced increases with Reynolds number between 800 and 2300. Figure 5 shows that there is an inverse relationship between pH and heat transfer coefficient. The reason is that the fluid used to raise the pH levels while producing nanomaterials; Since 25% is NH3 and 75% water, the specific heat of the fluid is lower than that of CuO nano fluids.
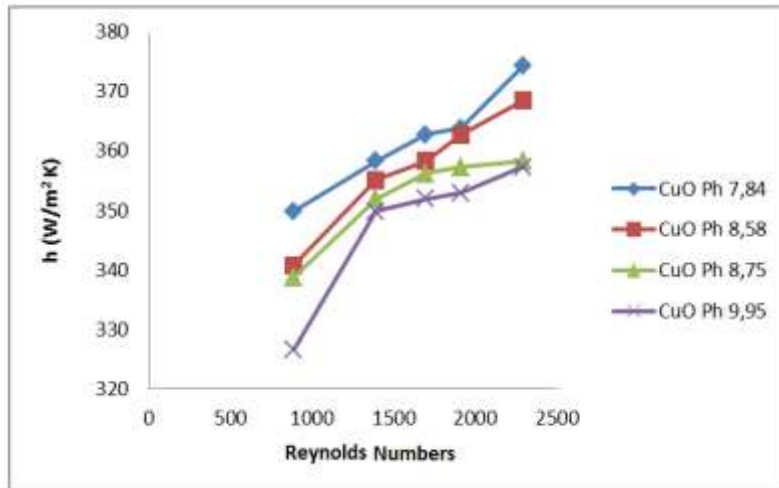
Fig. 5 Variation of heat transfer coefficient for CuO pH values by Reynolds number

3.1 SEM Images of Materials
The nanoparticle images at different pHs taken with the SEM display device are shown in Figure 6-9, respectively.
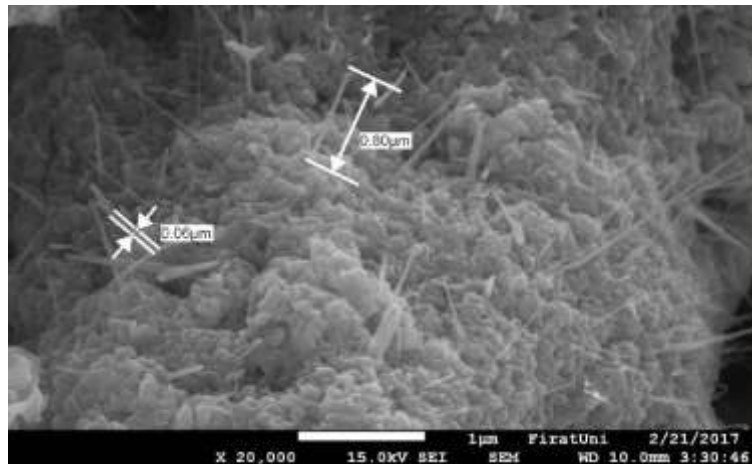

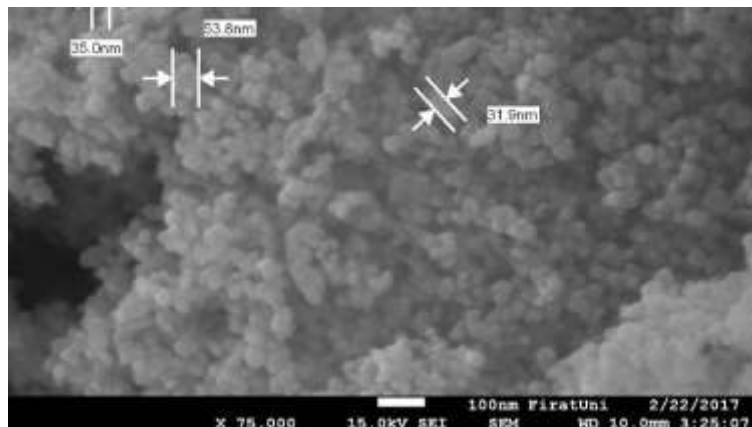**Fig. 6** SEM image of CuO pH 7 nanoparticle
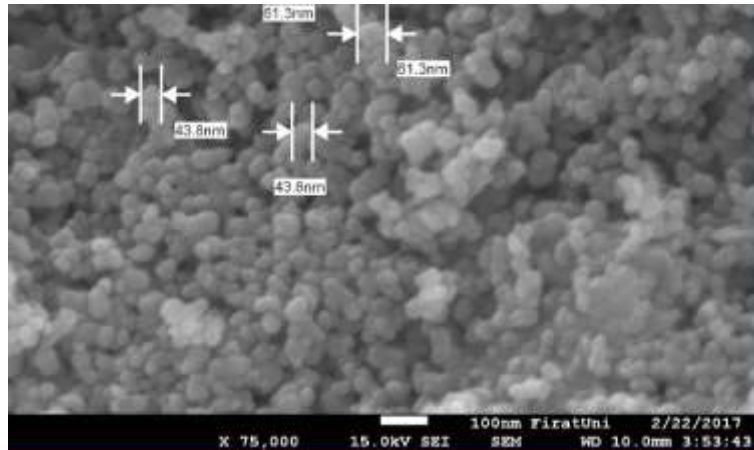

Fig. 7 SEM image of CuO pH 10 nanoparticle
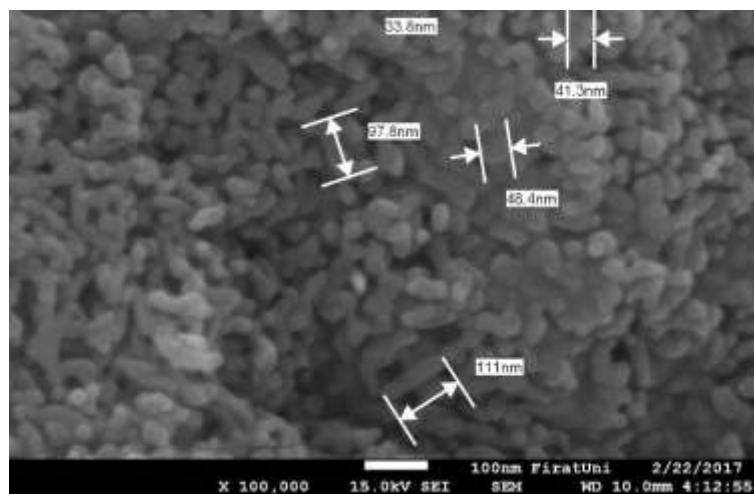
Fig. 8 SEM image of CuO pH 12 nanoparticle

Fig. 9 SEM image of CuO pH 14 nanoparticle

According to SEM analysis images in Figure 5-8, the morphological structure and dimensions of the CuO nanoparticles produced at various pHs were found to be successful in the production of nanoparticles.

3.2 UV Visible Reflection Analysis Results of Materials
The UV-visible reflection spectrum analyzes of the powdered samples are shown in Figure 10 and the optical absorption margins are homogeneous and the samples synthesized were confirmed to be pure CuO and no other vessel was detected.
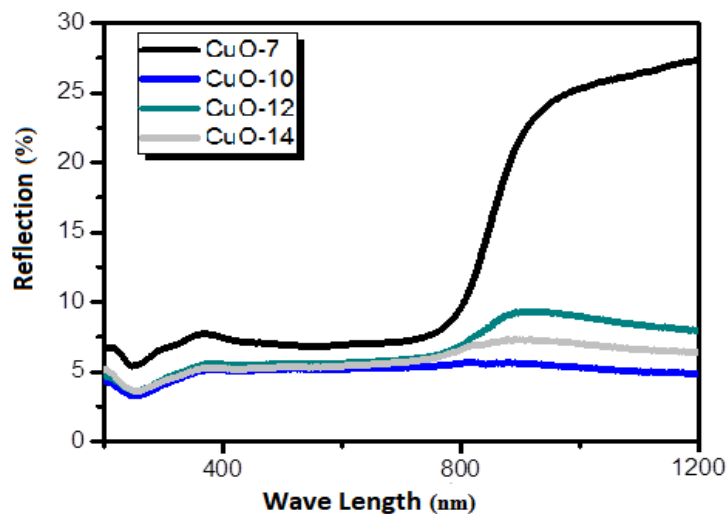

Fig. 10 UV-visible reflection spectra of powdered CuO nanoparticles

The examined graph of the band gap energy of the nanoparticle at different pH values of the solution is shown in Figure 11.
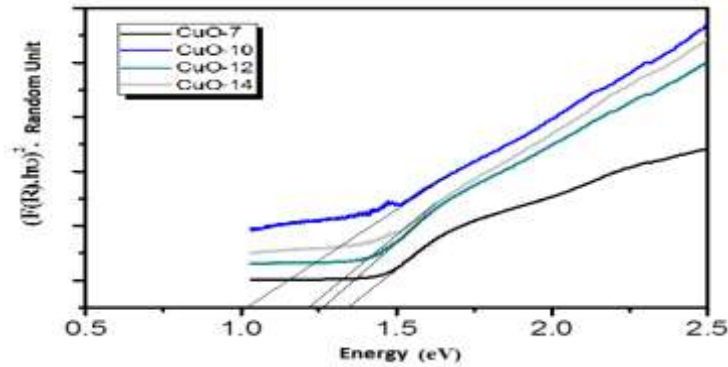

Fig.11 Demonstration of band gap energy of CuO nanoparticles at different pH values

The direct band gap energy of these materials was estimated using the Kubelka-Munk function. The Kubelka-Munk function formulation is given below.

$$(F(R)h\upsilon)^2 \alpha (h\upsilon - Eg) \qquad (6)$$

$$F(R) = \frac{(1-R)^2}{2R}$$

As shown in Figure 10, CuO nanoparticles have been found to be in the range of 1.02-1.35 eV at different pH values of the band gap energy solution. The CuO sample with pH 7 has the highest band gap energy of 1.35 eV. Eg (energy gap) change at different pH values is shown. The trend of change in ego values showed a change in morphology and a decrease in crystal size. The quantum limiting effect has played a major role in decreasing particle size and increasing band spacing.

3.3 Creating Predictive Models For H Values With Decision Tree Regression
The error rates for decision tree regression predicted model created for heat transfer coefficients of CuO nanofluids are shown in Table 2.

Tablo 2. Decision tree error rates

Error Analyze	Error Rate
MAE	0.9499
RMSE	0.971
RAE	33.5 %
RRAE	31.4 %

Figure 12 shows the h values estimated by the decision tree regression and the h values calculated from the experimental study.
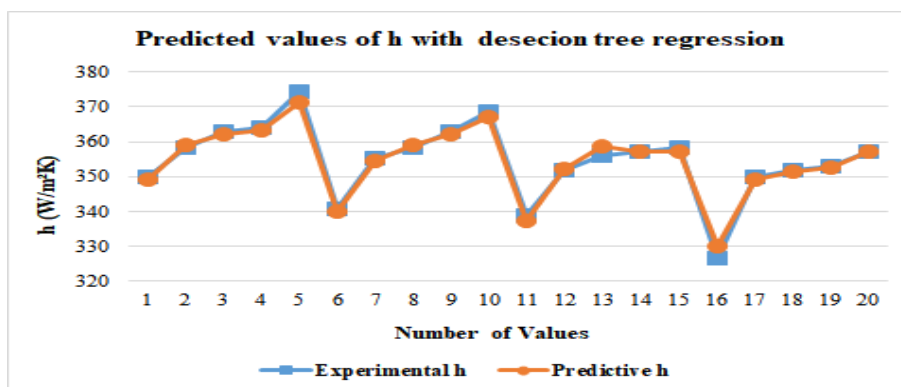

Fig. 12 Estimated h values obtained using decision tree regression

IV.   CONCLUSION

Our work, SEM image measurements and Ultra-violet visible light (UV-Vis) analysis of the particles produced after the production of CuO nanoparticles has been shown to be successful in the production of nanoparticles. CuO nanoparticles were produced. Heat transfer coefficients were calculated by using the

nanoparticles produced by using pure water, ethanol and ethylene glycol material with the nanoparticles produced. As the Reynolds number increased, the heat transfer coefficient of nano fulids increased in accordance with the calculations. When the pH values increased, it was observed that the heat transfer coefficient of the nano fluids decreased. When the values in Figure 4 are transferred to Table 3, this change is seen more clearly.

Table 3. Change of heat transfer values of CuO nano fluid

Re	CuO 7.84(h)	CuO 8.58(h)	CuO 8.75(h)	CuO 9.95(h)
887	349,821	340,722	338,764	326,565
1391	358,328	355,090	351,910	349,821
1695	362,738	358,328	356,163	351,910
1912	363,857	362,738	357,242	352,963
2290	374,253	368,406	358,328	357,242

The network has been trained to improve the predictive ability of decision tree regression. The predicted and the actual measured h values are similar. It was concluded that for the predictive model of h is a successful modeling according to the error analysis results of decision tree regression (Table 2). As shown in Figure 11, the experimental and predictive h values are very close to each other. More successful prediction models can be obtained by using different computational intelligence methods.

Acknowledgements

REFERENCES

[1]. Abraham J.P., Sparrow Tong. J.C.K., Bettenhausen. D.W. Internal flows which transist from turbulent through intermittent to laminar. International Journal of Thermal Sciences. 49. 256–263, 2010.
[2]. Maxwell J. C., A Treatise on Electricity and Magnetism, (Clarendon Press, Oxford, UK, Second ed.,1881).
[3]. Gürmen, S. Ebin, B. Nanoparticles and Production Methods-1, Metallurgical Journal, 150, 31-38, 2008.
[4]. Xuan Y., Li Q. Heat transfer enhancement of nanofluids, International Journal of Heat and Fluid Flow, 21(1), 58–64, 2000.
[5]. Choi, S.U.S. Enhancing thermal conductivity of fluids with nanoparticles, The Proceedings of the 1995 ASME International Mechanical Engineering Congress and Exposition, San Francisco, USA, ASME, FED 231/MD 66, 99–105, 1995.
[6]. Zhu, H., Lin, Y., Yin, Y. A novel one-step chemical method for preparation of copper nanofluids, Journal of Colloid and Interface Science, 277, 100–103, 2004.
[7]. Eastman, J. A., Choi, S. U. S., Li, S., Yu,W., Thompson, L. J. Anomalously Increased Effective Thermal Conductivity of Ethylene Glycol-Based Nanofluids Containing Copper Nanoparticles, Applied Physics Letters, 78, 718–720 (2001)
[8]. Chang, H., Tsung, T. T., Chen, L. C., Yang, Y. C., Lin, H. M., Lin, C. K., Jwo, C. S. Nanoparticle Suspension Preparation Using the Arc Spray Nanoparticle Synthesis System Combined with Ultrasonic Vibration and Rotating Electrode, The International Journal of Advanced Manufacturing Technology, 26, 552–558 (2005).
[9]. Kumar V., Tiwari A., Ghosh S., Application of Nanofluids in Plate Heat Exchanger: A Review, Energy Conversion and Management 105: 1017-1036 (2005).
[10]. Nguyen, C.T., Desgranges F., Gilles R., Nicolas G., Thierry M., Boucher S. Temperature and particle-size dependent viscosity data for water-based nanofluids–hysteresis phenomenon, Int. J. Heat Fluid Flow, 28(6), 1492– 1506 (2007).
[11]. Gonçalves, J. S. V., Santos, S. H. and Leal, L. S. Santos Junior1, M. R. M. C. Santos1, E. Longo and Matos, J. M. E. ,Experimental variables in the synthesis of anatase phase TiO2 nanoparticles, 11th International Conference on Advanced Materials, Rio de janeiro Brazil (2009).
[12]. 16. Xie H, Wang J, Xi T, Liu Y. Study on the thermal conductivity of SiC nanofluids. J Chin Ceram Soc, 29(4), 361–364 (2001).
[13]. Elmas, Ç., 2003. Artificial Neural Network, Seçkin Publishing House, Ankara, Turkey.
[14]. Uysal, C., Korkmaz, M. E. Estimation of entropy generation for Ag-MgO/water hybrid nanofluid flow through rectangular minichannel by using artificial neural network. Politeknik Dergisi, ISSN: 2147-9429 (2018).
[15]. Kılıç, M., Yavuz, M., Yılmaz, İ. H. Numerical investigation of combined effect of nanofluids and impinging jets on heated surface. International Advanced Researches and Engineering Journal, 2(1), 14-19 (2018).
[16]. Çengel Yunus A., Practical Approach to Heat and Mass Transfer (McGraw Hill**,** 3rd Edition, 467- 468 (2010).
[17]. Gil, E., et al. XPS and SEM analysis of the surface of gas atomized powder precursor of ODS ferritic steels obtained through the STARS route. Applied Surface Science, 427: 182-191, 2018.
[18]. Karoui, R. Spectroscopic Technique: Fluorescence and Ultraviolet-Visible (UV-Vis) Spectroscopies. In: Modern techniques for food authentication. Academic Press, p. 219-252, 2018.
[19]. Safavian S.R., Landgrebe D., "A survey of decision tree classifier methodology", IEEE Transactions on Systems Man and Cybernetics, 21, 660-674, 1991.
[20]. Pal M., Mather P.M., "An assessment of the effectiveness of decision tree methods for land cover classification", Remote Sensing of Environment, 86, 554-565, 2003.